

Topological magnon: Weyl magnons in ordered antiferromagnet

Gang Chen
Fudan University



Outline

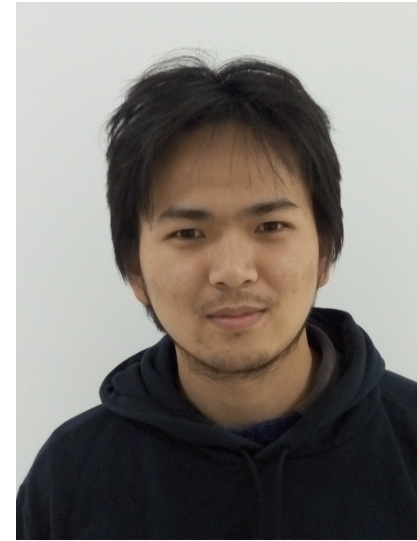
1. Introduction to Weyl semimetal
2. Antiferromagnet and spin waves
3. Generalities and uniqueness of Topological (Weyl) magnon

it is a student project !
it is a simple piece of work, there is
Not much creativity !

Collaborators



Fei-Ye Li (Fudan)
李非也



Yaodong Li (Fudan->UCSB)

and Yue Yu, Leon Balents, YongBaek Kim

Fei-Ye Li, Yao-dong Li ... **Gang Chen***, Nature Comms.

 Selected for a [Viewpoint](#) in *Physics*

PHYSICAL REVIEW B **83**, 205101 (2011)



Topological semimetal and Fermi-arc surface states in the electronic structure of pyrochlore iridates

Xiangang Wan,¹ Ari M. Turner,² Ashvin Vishwanath,^{2,3} and Sergey Y. Savrasov^{1,4}

¹*National Laboratory of Solid State Microstructures and Department of Physics, Nanjing University, Nanjing 210093, China*

²*Department of Physics, University of California, Berkeley, California 94720, USA*

³*Materials Sciences Division, Lawrence Berkeley National Laboratory, Berkeley, California 94720, USA*

⁴*Department of Physics, University of California, Davis, One Shields Avenue, Davis, California 95616, USA*

(Received 23 February 2011; published 2 May 2011)

Physics

Physics **4**, 36 (2011)

Viewpoint

Weyl electrons kiss

Leon Balents

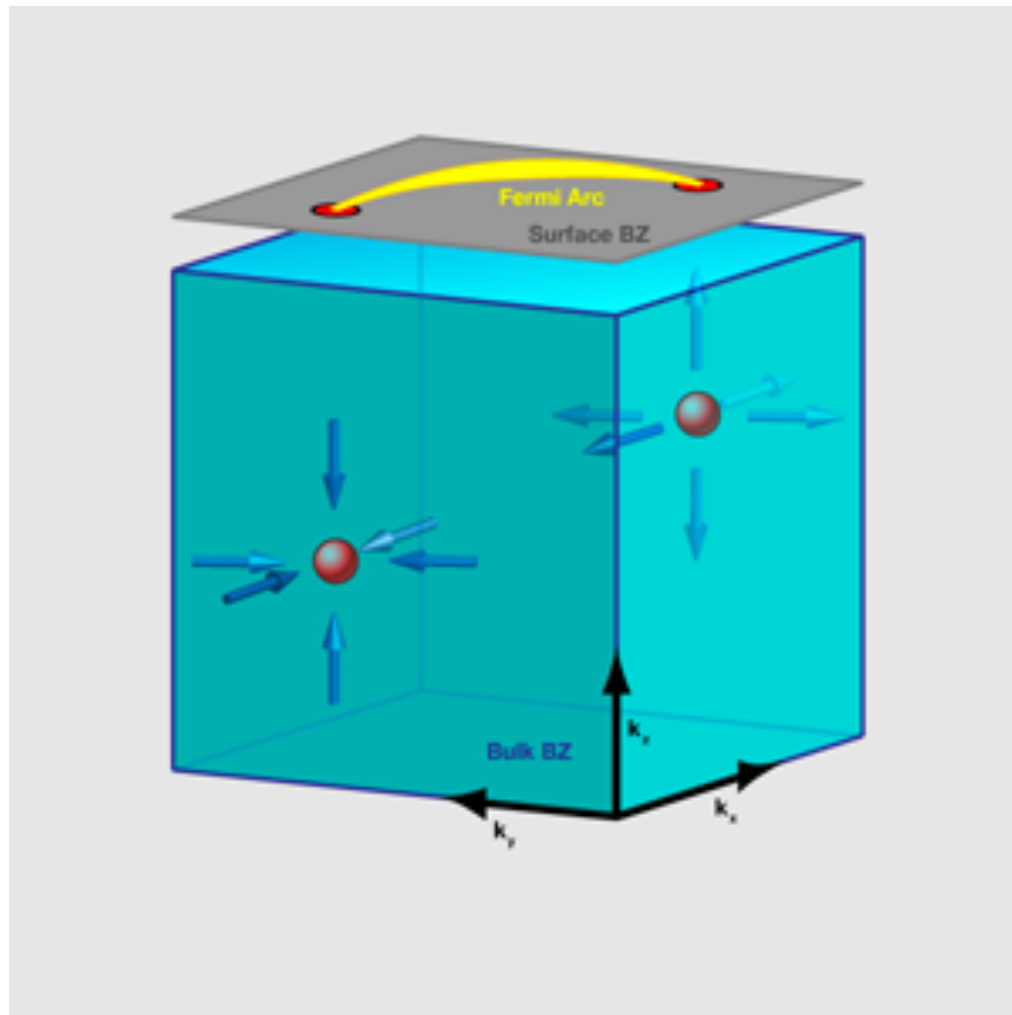
Kavli Institute for Theoretical Physics, University of California, Santa Barbara, CA 93106, USA

Published May 2, 2011

Theorists predict the possibility of topological “Fermi arc” surface states in a system with broken time-reversal symmetry.

Subject Areas: **Strongly Correlated Materials**

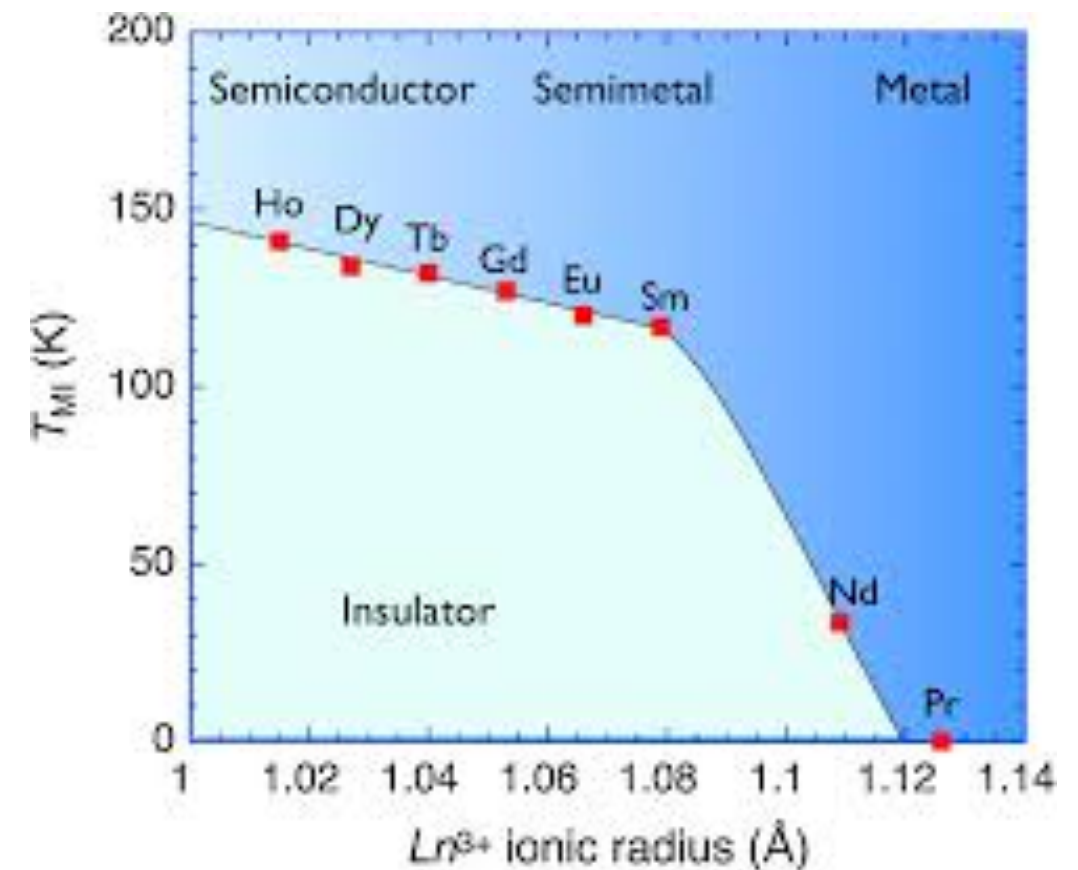
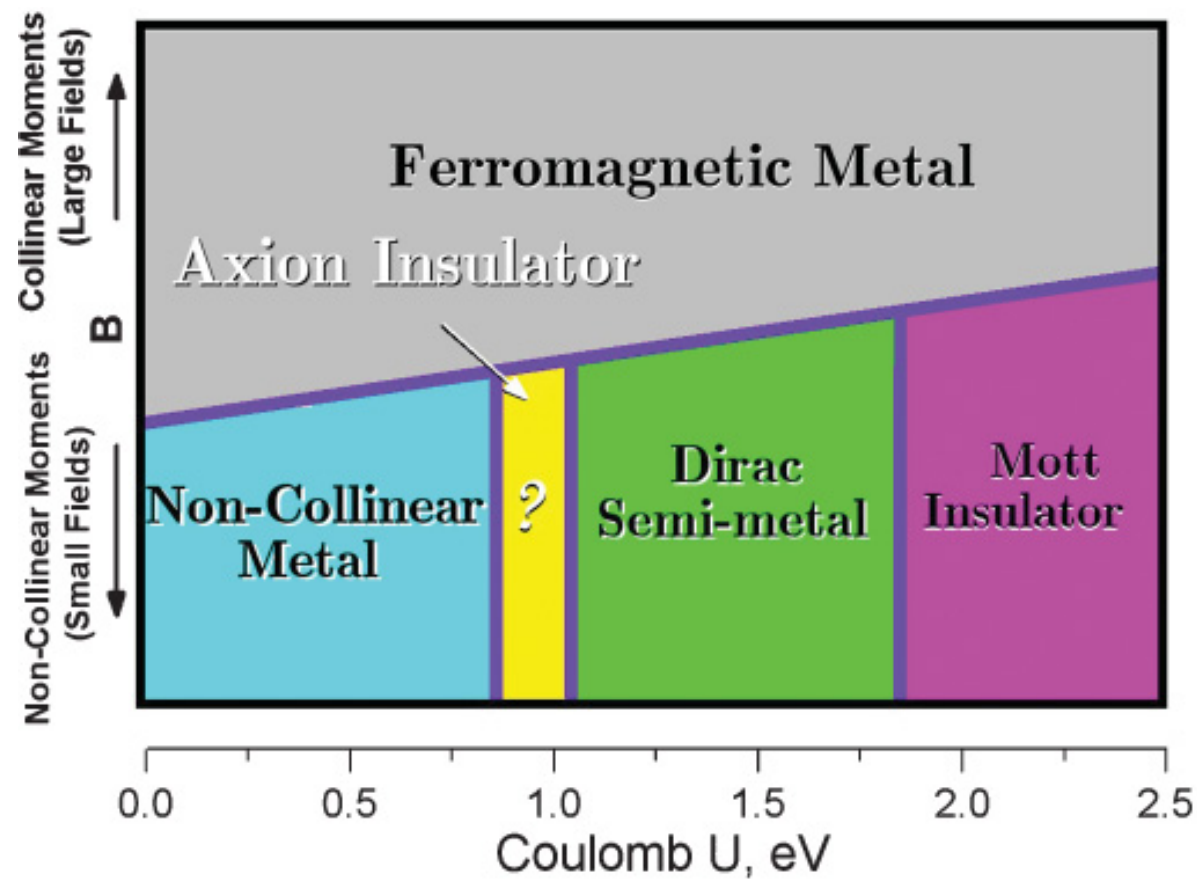
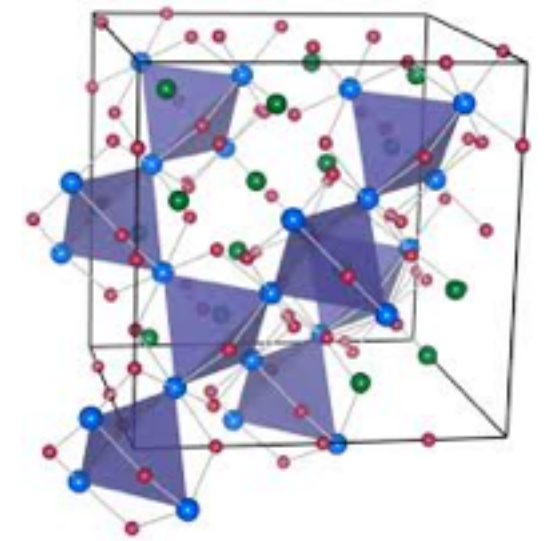
Weyl semimetal



$$H_D = E_0 \mathbb{1} + \mathbf{v}_0 \cdot \mathbf{q} \mathbb{1} + \sum_{i=1}^3 \mathbf{v}_i \cdot \mathbf{q} \sigma_i. \quad (1)$$

Energy is measured from the chemical potential, $\mathbf{q} = \mathbf{k} - \mathbf{k}_0$

Weyl semimetal proposed in pyrochlore iridates



Xiangang Wan, Turner, Vishwanath, Savrasov, PhysRevB 2011,
Magnetic Weyl semimetal from the Ir correlation driven all-in all-out order.

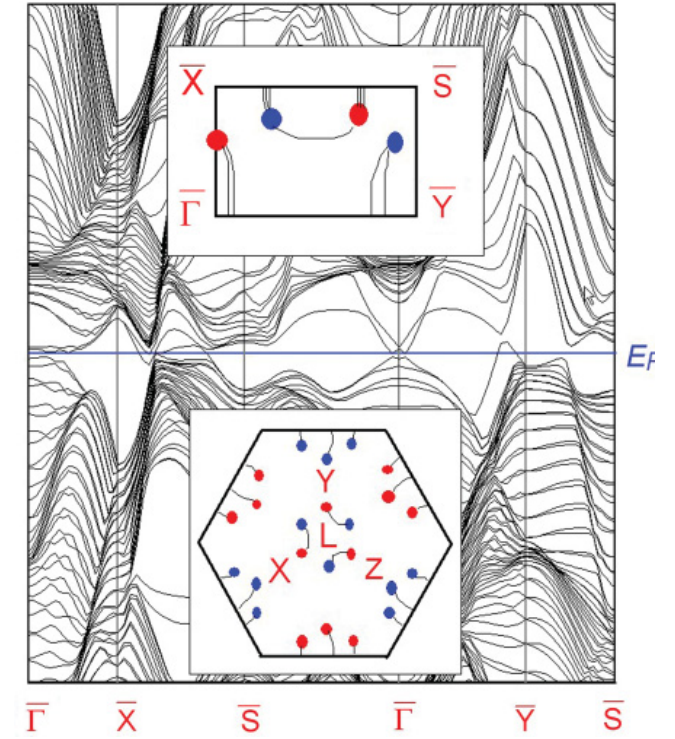
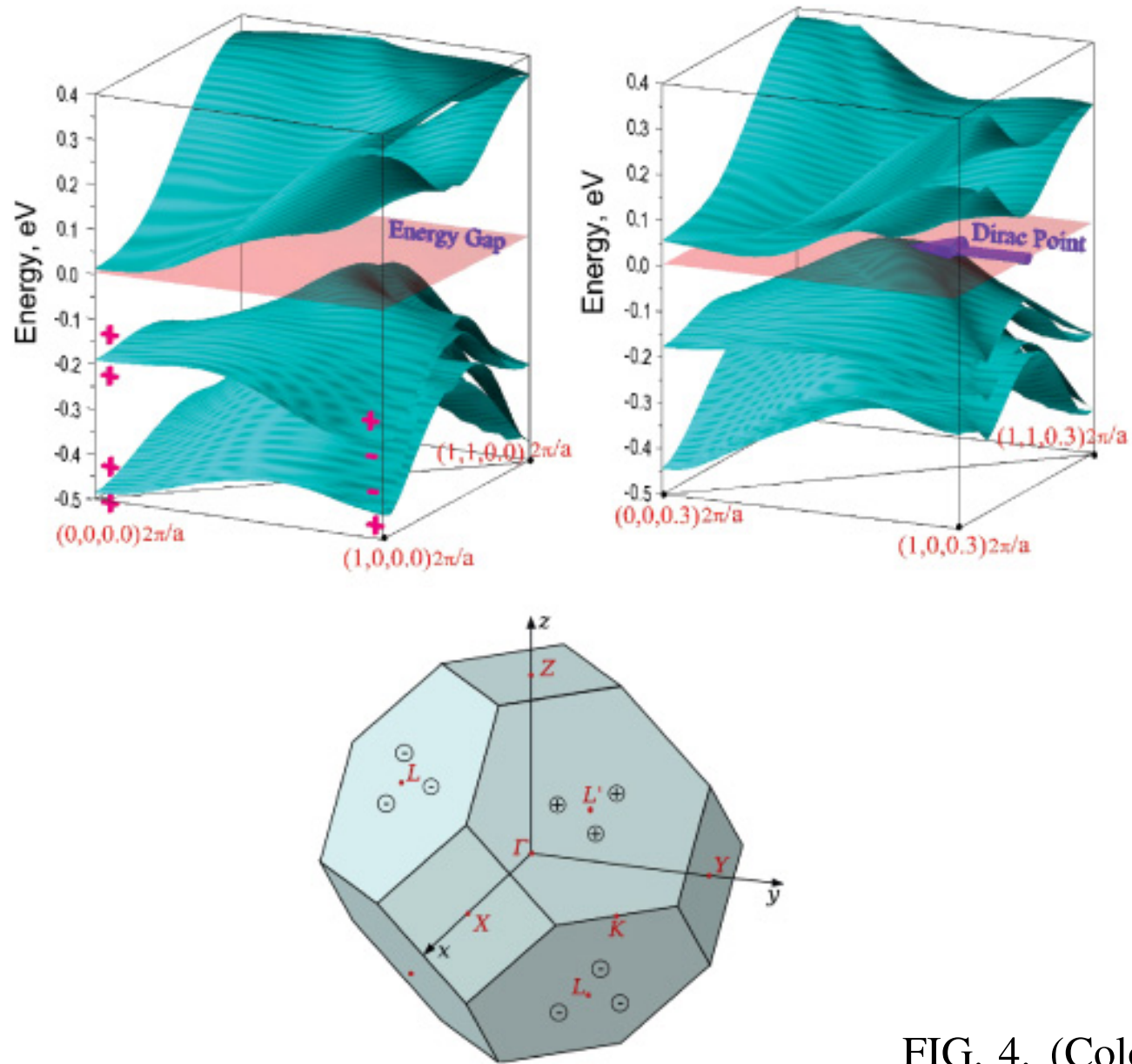


FIG. 4. (Color online) Semimetallic nature of the state at $U = 1.5$ eV according to the LSDA + U + SO method. (a) Calculated energy bands in the plane $K_z = 0$ with band parities shown; (b) energy bands in the plane $k_z = 0.6\pi/a$, where a Weyl point is predicted to exist. The lighter-shaded plane is at the Fermi level. (c) Locations of the Weyl points in the three-dimensional Brillouin zone (Ref. 29) (nine are shown, indicated by the circled + or - signs).

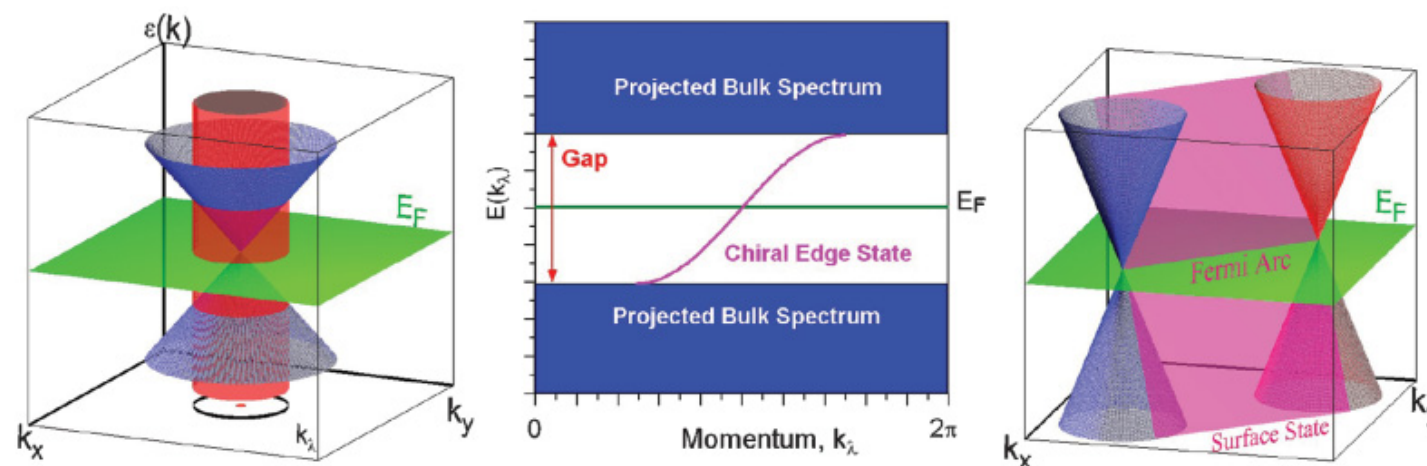


FIG. 5. (Color online) Illustration of surface states arising from bulk Weyl points. (a) The bulk states as a function of (k_x, k_y) (and arbitrary k_z) fill the inside of a cone. A cylinder whose base defines a one-dimensional circular Brillouin zone is also drawn. (b) The cylinder unrolled onto a plane gives the spectrum of the two-dimensional subsystem $H(\lambda, k_z)$ with a boundary. On top of the bulk spectrum, a chiral state appears due to the nonzero Chern number. (c) Meaning of the surface states back in the three-dimensional system. The chiral state appears as a surface connecting the original Dirac cone to a second one, and the intersection between this plane and the Fermi level gives a Fermi arc connecting the Weyl points.

The Weyl points behave like “magnetic” monopoles in momentum space whose charge is given by the chirality; they are actually a source of “Berry flux” rather than magnetic flux. The Berry connection, a vector potential in momentum space, is defined by $\mathcal{A}(\mathbf{k}) = \sum_{n=1}^N i \langle u_{n\mathbf{k}} | \nabla_{\mathbf{k}} | u_{n\mathbf{k}} \rangle$, where N is the number of occupied bands. As usual, the Berry flux is defined as $\mathcal{F} = \nabla_{\mathbf{k}} \times \mathcal{A}$. To show that there are arcs connecting pairs of Weyl points, we argue that there is an arc on the surface Brillouin zone emanating from the projection (k_{0x}, k_{0y}) of each Weyl point.

Chirality and Types of Weyl nodes

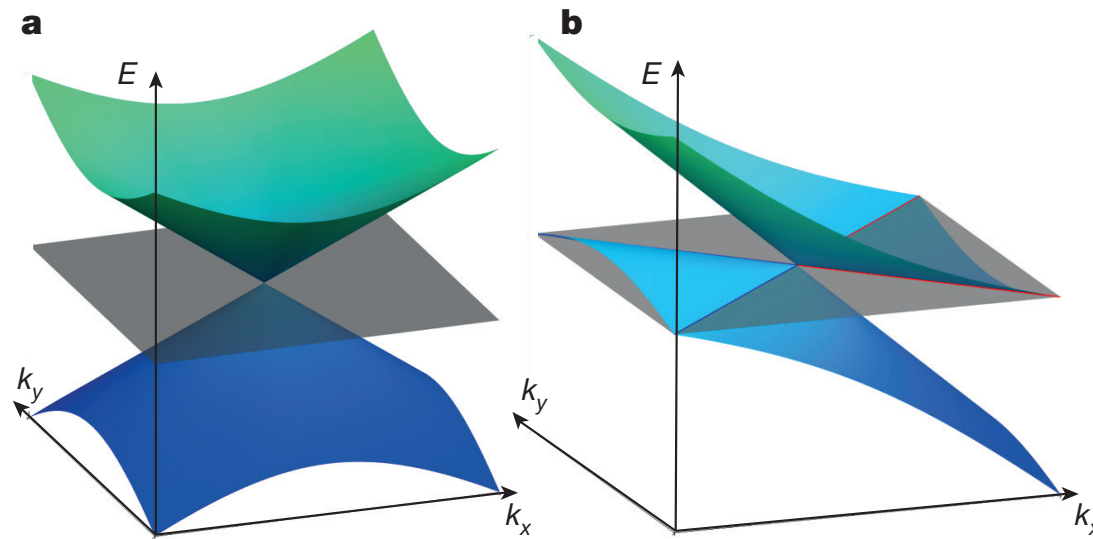


Figure 1 | Possible types of Weyl semimetals. **a**, Type-I WP with a point-like Fermi surface. **b**, A type-II WP appears as the contact point between electron and hole pockets. The grey plane corresponds to the position of the Fermi level, and the blue (red) lines mark the boundaries of the hole (electron) pockets.

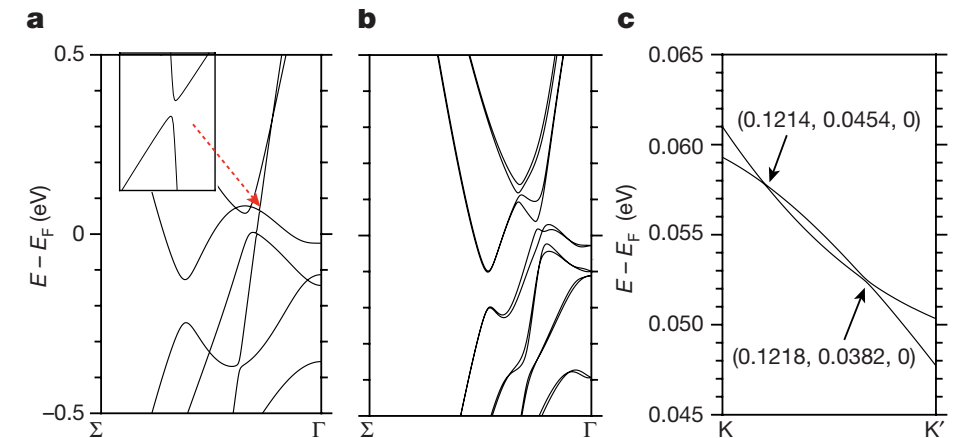


Figure 2 | Band structure of WTe₂. **a**, Band structure of WTe₂ without SOC. A fraction of the Γ -X segment is shown: the point Σ has coordinates (0.375, 0, 0). A bandgap of approximately 1 meV is shown in the inset, signalling a gapless point nearby. **b**, Band structure of WTe₂ with SOC. **c**, One of the four pairs of WPs is shown along the line K-K', where $K = (0.1208, 0.0562, 0)$ and $K' = (0.1226, 0.0238, 0)$. Their locations are designated in reduced coordinates (in units of reciprocal lattice constants).

Type-II Weyl semimetals

Alexey A. Soluyanov¹, Dominik Gresch¹, Zhijun Wang², QuanSheng Wu¹, Matthias Troyer¹, Xi Dai³ & B. Andrei Bernevig²

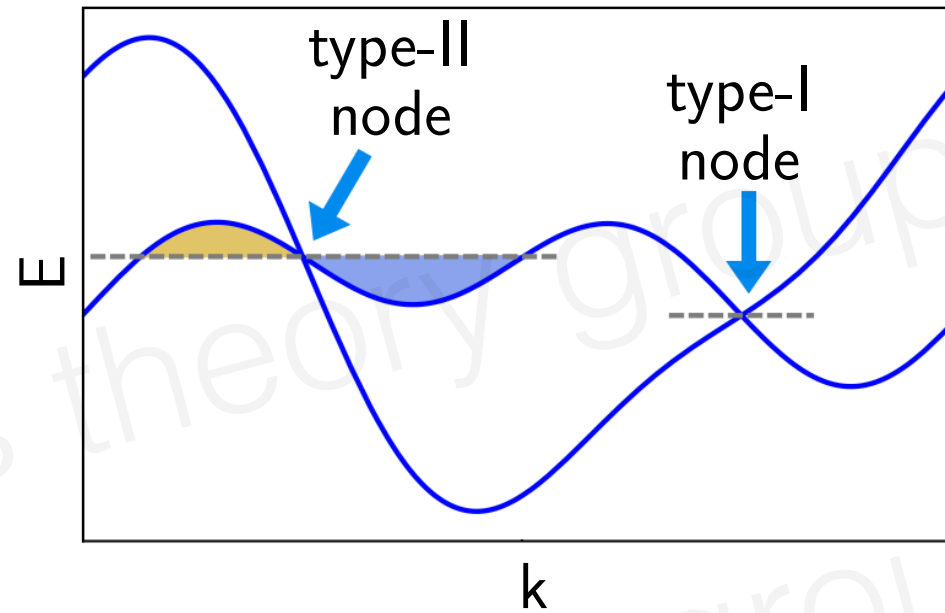
Hybrid Weyl Semimetal

Fei-Ye Li^{1,*} Xi Luo^{1,*} Xi Dai², Yue Yu^{3,5}, Fan Zhang⁴, and Gang Chen^{3,5†}



Fei-Ye Li

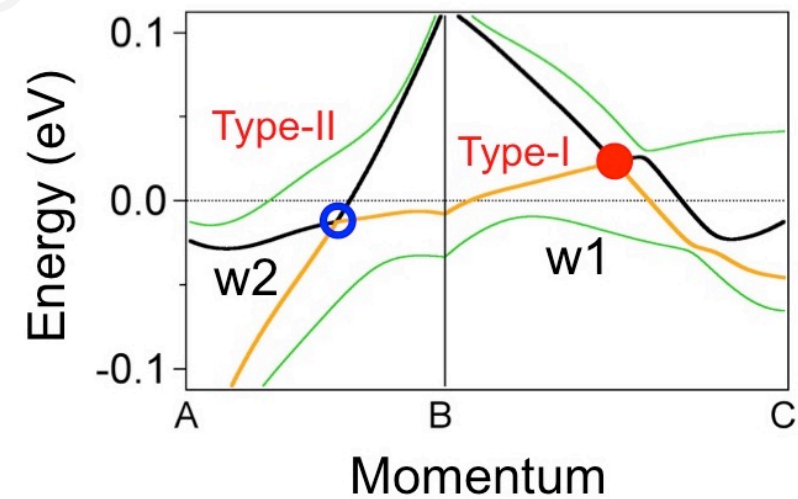
PRB 94,121105 (2016)



chirality is topological, type is local.

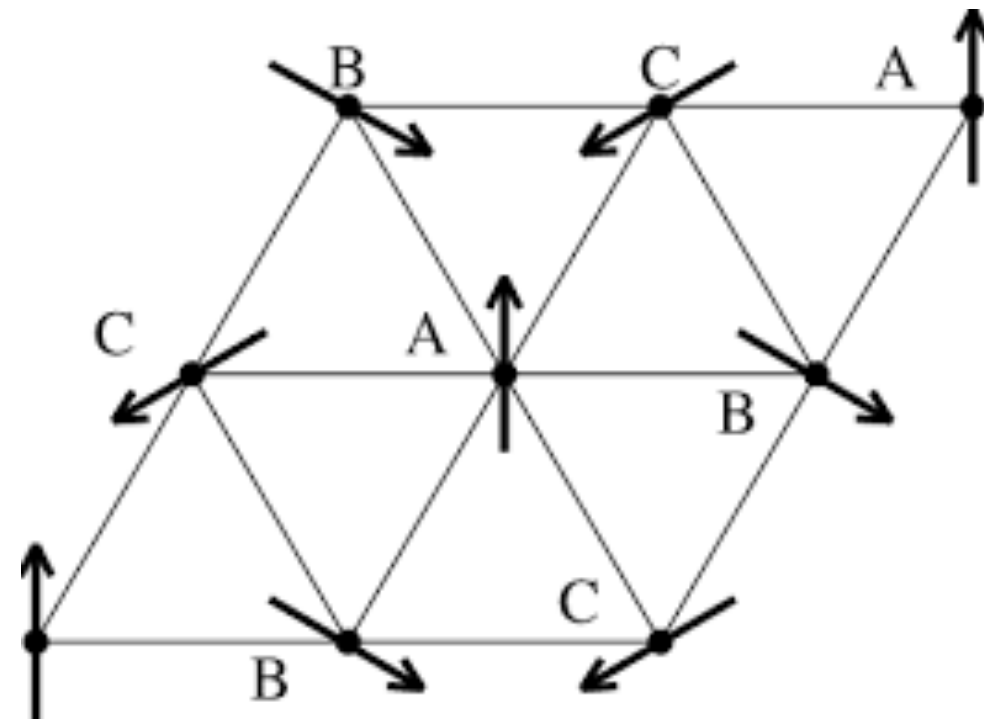
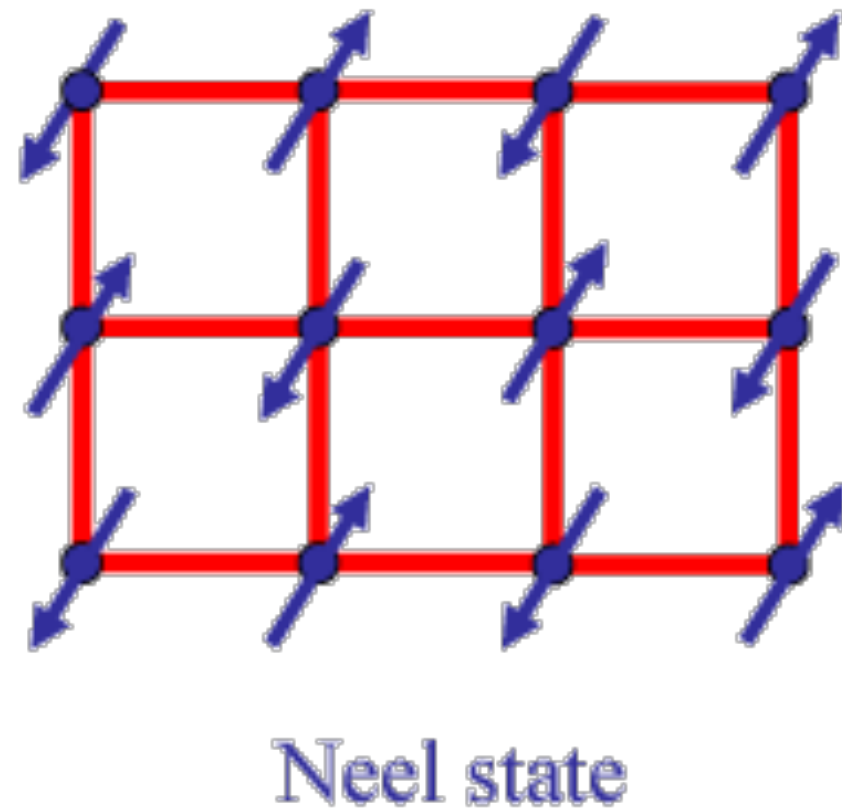
Evidence of Coulomb interaction induced Lifshitz transition and robust hybrid Weyl semimetal in T_d MoTe₂

N. Xu^{1,*}, Z. W. Wang², A. Magrez³, P. Bugnon³, H. Berger³, C. E. Matt^{4,5}, V. N. Strocov⁴, N. C. Plumb⁴, M. Radovic⁴, E. Pomjakushina⁶, K. Conder⁶, J. H. Dil^{3,4}, J. Mesot^{3,4,5}, R. Yu², H. Ding^{7,8,*} and M. Shi^{4,*}



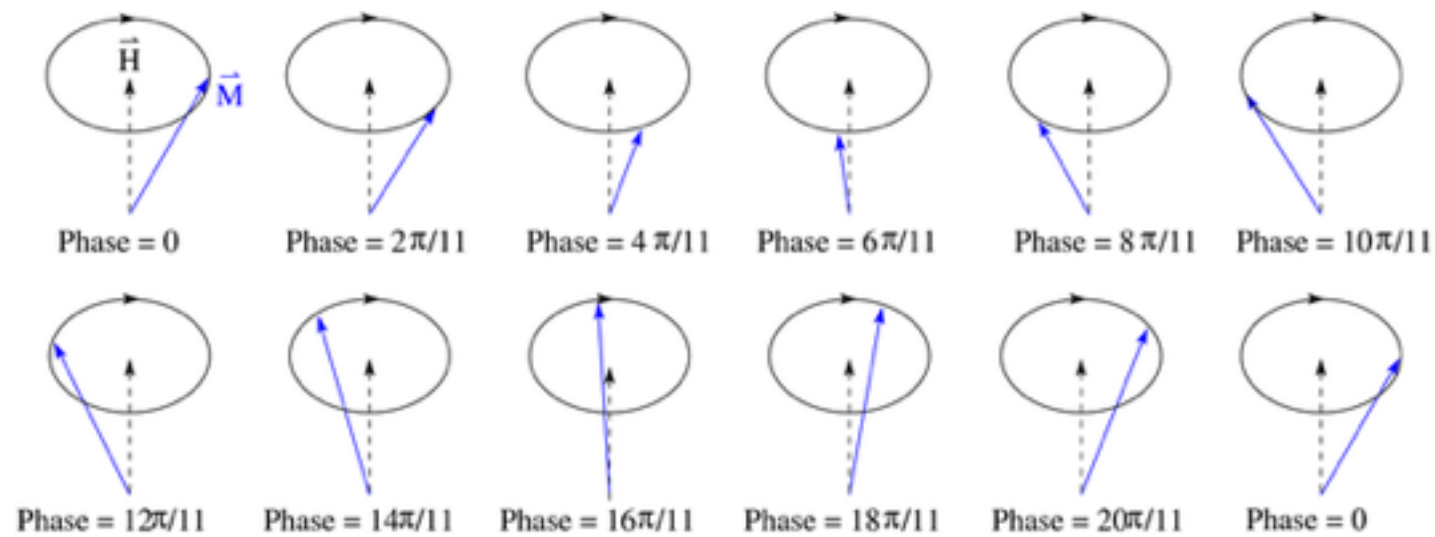
2. Antiferromagnet and spin waves

Ordered AFMs



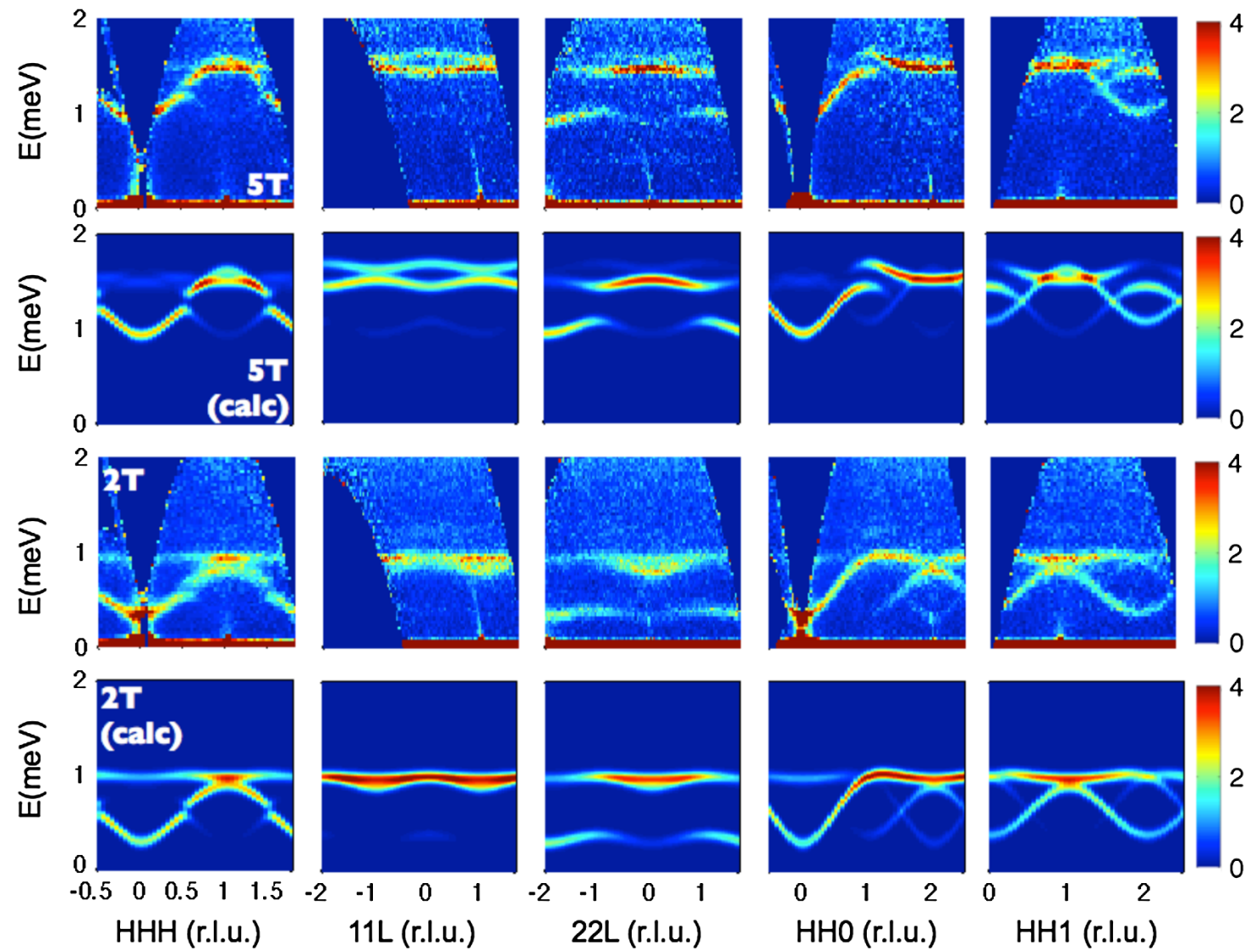
Ground state orders for AFMagnetic Heisenberg model

Propagating spin waves and Holstein-Primakoff spin wave



$$S_+ = \hbar\sqrt{2s}\sqrt{1 - \frac{a^\dagger a}{2s}} a, \quad S_- = \hbar\sqrt{2s}a^\dagger \sqrt{1 - \frac{a^\dagger a}{2s}}, \quad S_z = \hbar(s - a^\dagger a).$$

An example of spin wave excitation in ordered AFM



Kate A. Ross,¹ Lucile Savary,² Bruce D. Gaulin,^{1,3,4} and Leon Balents^{5,*}

PHYSICAL REVIEW X **1**, 021002 (2011)

3. Weyl magnons in ordered antiferromagnet



P W Anderson

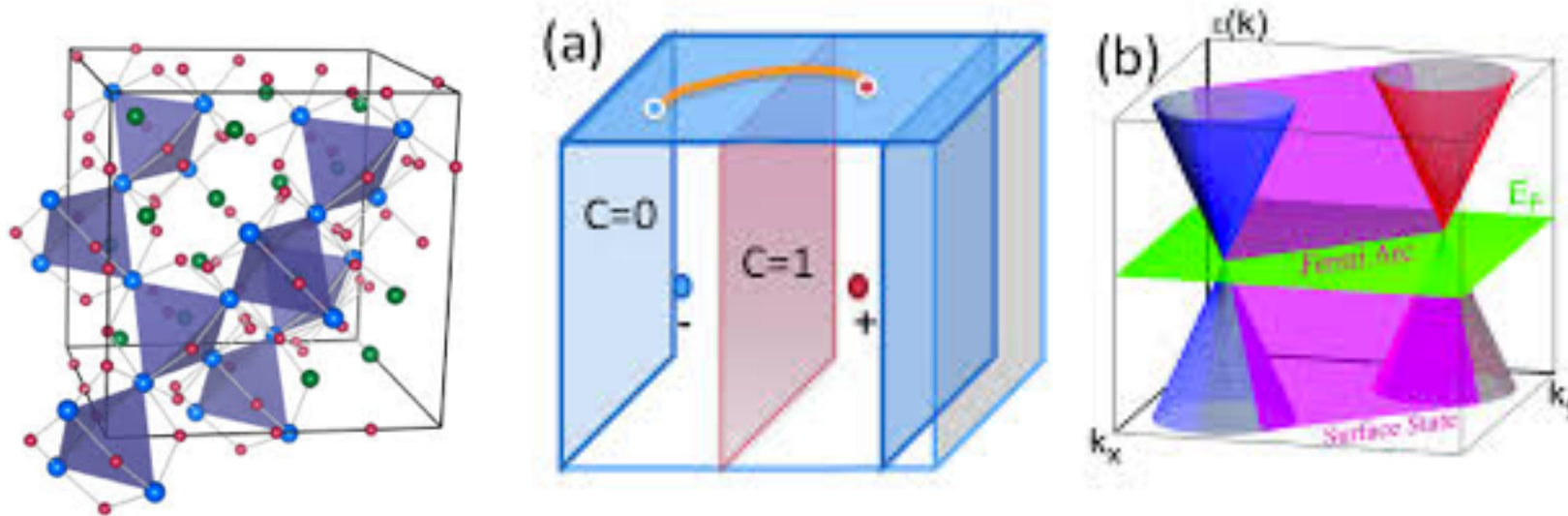


1984

“By Landau’s definition this is simply any parameter that is zero in the symmetric state and **has a nonzero average uniquely specifying the state** when the symmetry is broken.”

explain the history

Weyl fermions



Xiangang Wan, Vishwanath, et al 2011,
Burkov, Balents 2011

Hong Ding, Hasan, Ling Lu, Hongming Weng, **Xi Dai, Zhong Fang**, et al

Discovered in 2015 in various physical systems !

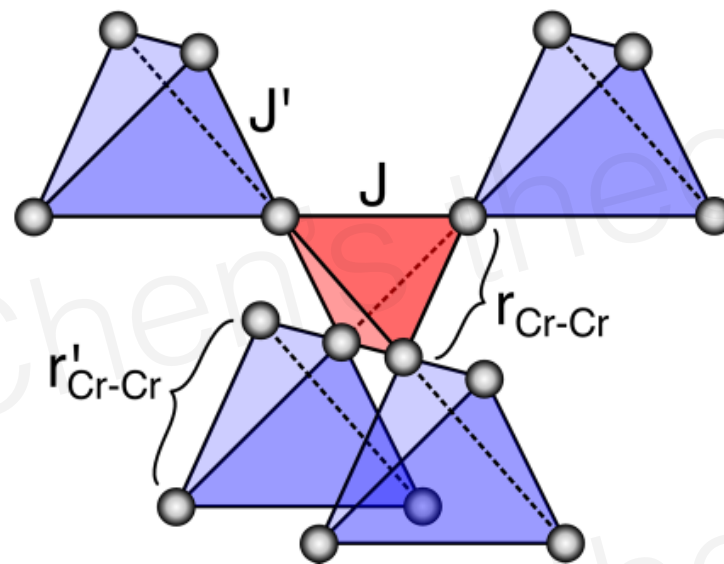
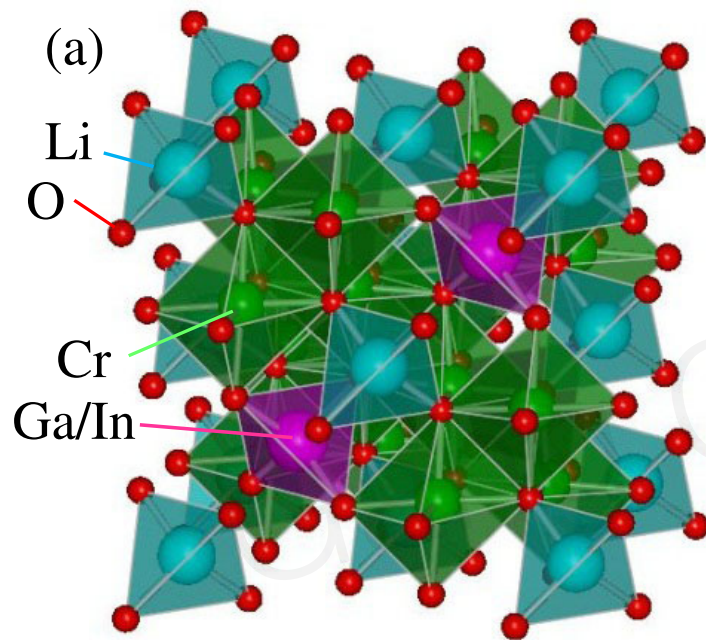
Remark

Weyl band touching is a **topological** property of the band structure, and is thus **independent** from the particle statistics.

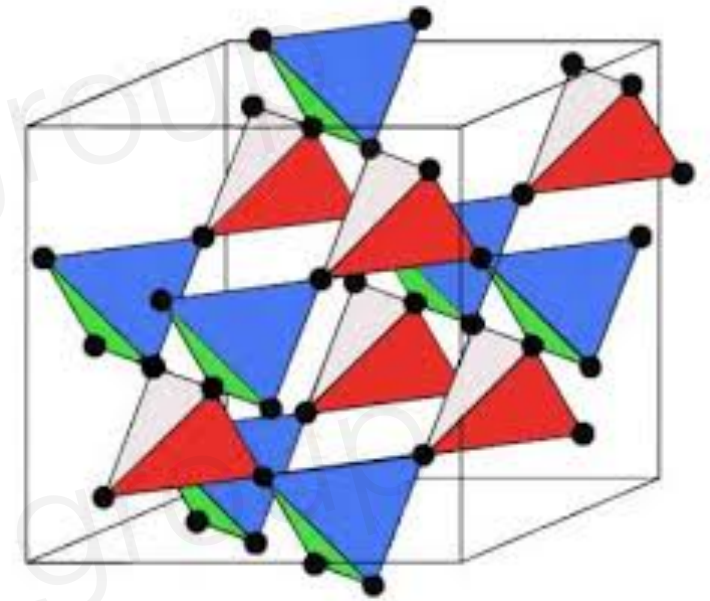
It can be fermion, e.g. electron, can also be boson, e.g. photon.

类似于 breathing

Breathing Pyrochlore



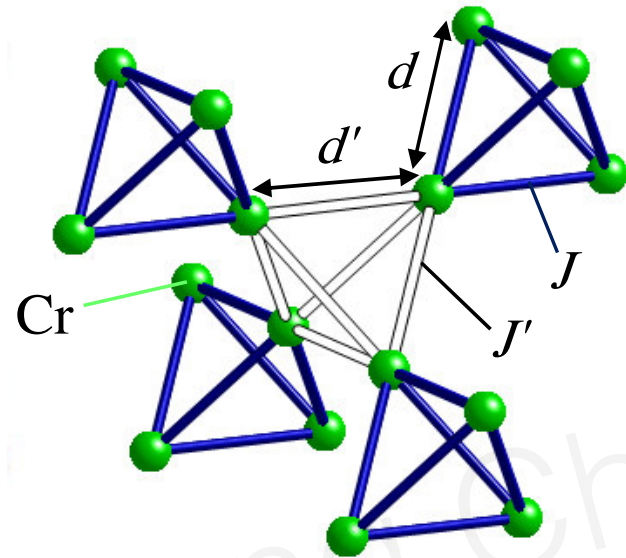
Breathing Pyrochlore



Regular Pyrochlore

K. Kimura, S. Nakatsuji, and T. Kimura, **PhysRevB** 2014,
Yoshihiko Okamoto, Gørn J. Nilsen, J. Paul Attfield, and Zenji Hiroi, **PhysRevLett** 2013,
Yu Tanaka, Makoto Yoshida, Masashi Takigawa, Yoshi- hiko Okamoto, and Zenji Hiroi, **PhysRevLett** 2014.

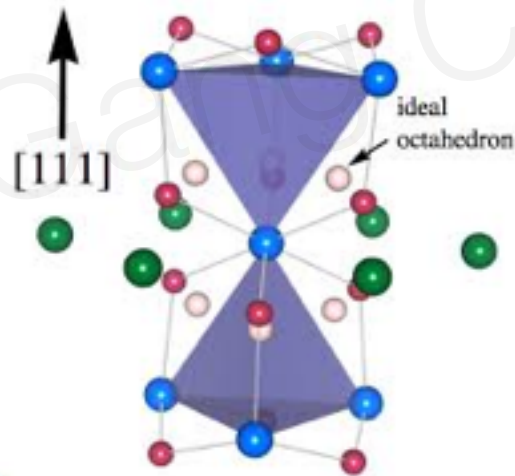
Minimal model and ground states



As there is no orbital degeneracy for the $3d^3$ electron configuration of Cr^{3+} ions, the orbital angular momentum is fully quenched and the Cr^{3+} local moment is well described by the total spin $S = 3/2$ via the Hund's rule. As

$$H = J \sum_{\langle ij \rangle \in \text{u}} \mathbf{S}_i \cdot \mathbf{S}_j + J' \sum_{\langle ij \rangle \in \text{d}} \mathbf{S}_i \cdot \mathbf{S}_j + D \sum_i (\mathbf{S}_i \cdot \hat{z}_i)^2,$$

Treating spins as classical vectors, simple algebra gives some rules for ground states



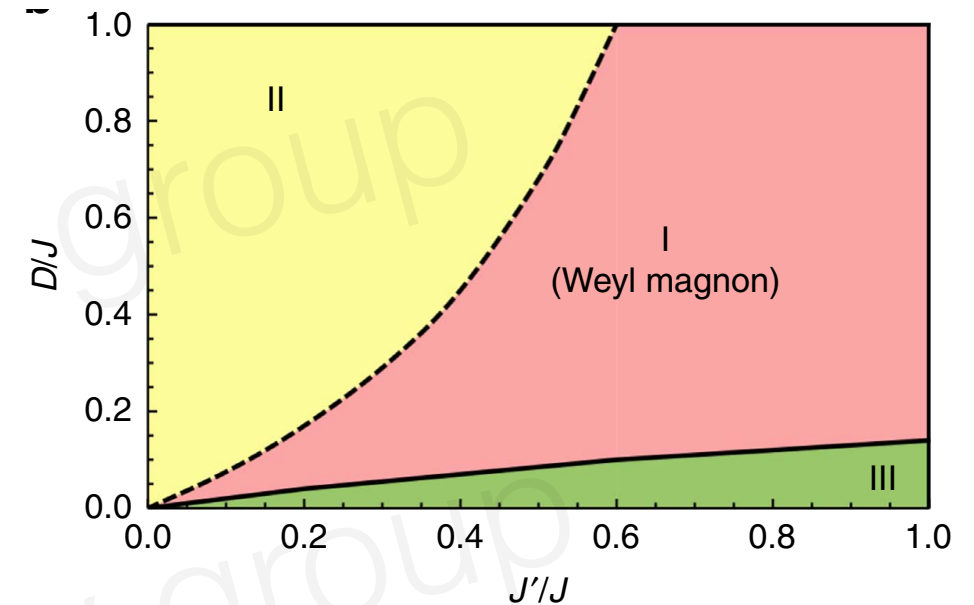
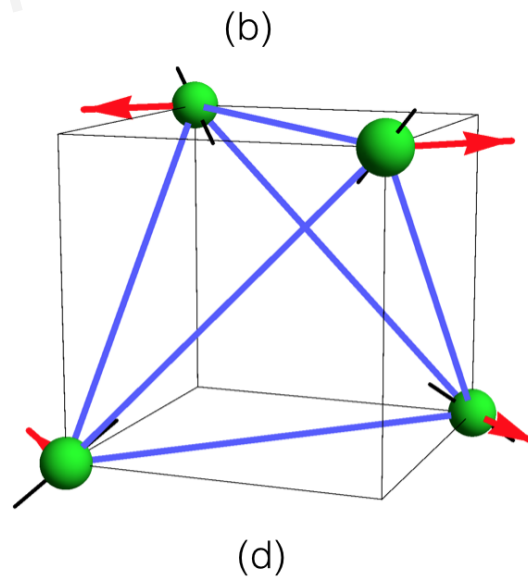
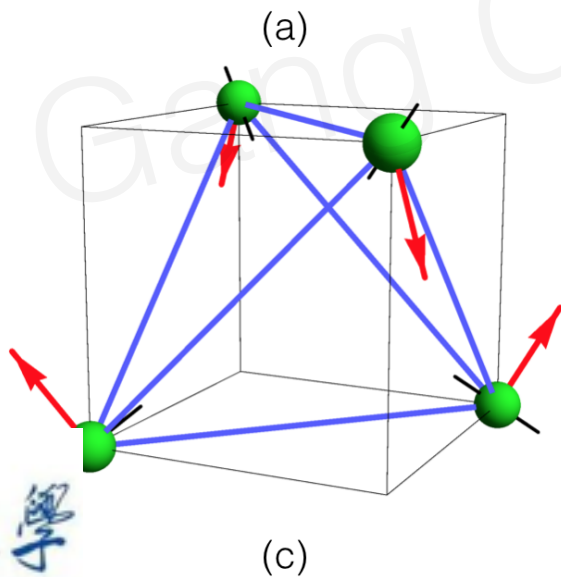
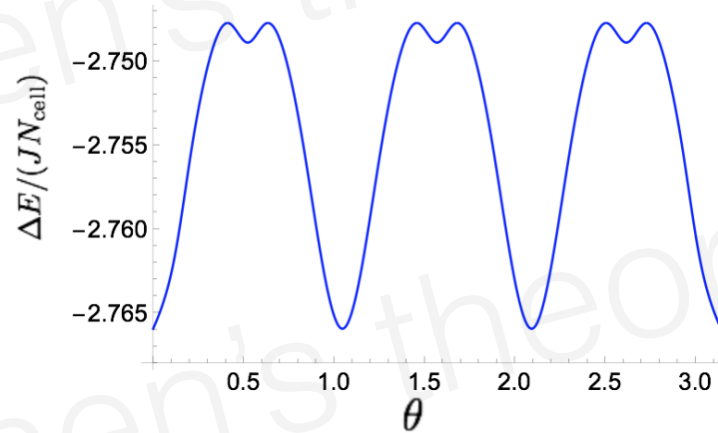
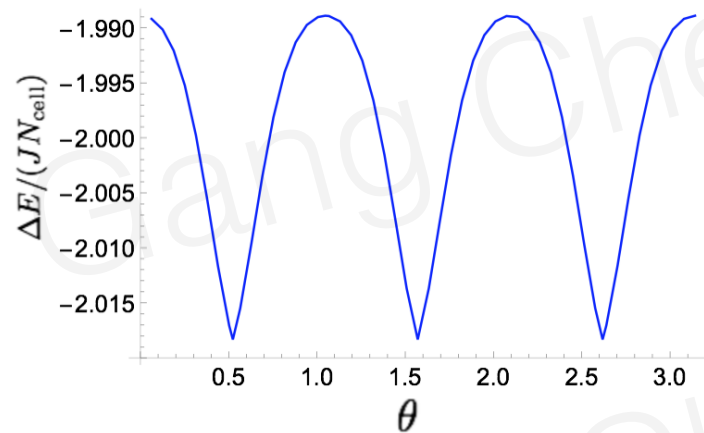
$$\sum_{\langle ij \rangle \in \text{u}} \mathbf{S}_i \cdot \mathbf{S}_j \sim \frac{1}{2} \left(\sum_{i \in \text{u}} \mathbf{S}_i \right)^2$$

$$\sum_{\langle ij \rangle \in \text{d}} \mathbf{S}_i \cdot \mathbf{S}_j \sim \frac{1}{2} \left(\sum_{i \in \text{d}} \mathbf{S}_i \right)^2$$

Quantum order by disorder

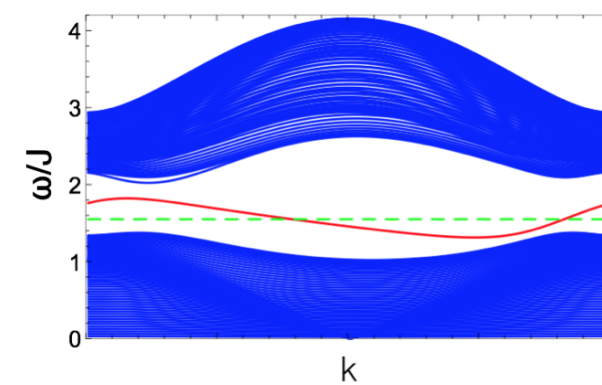
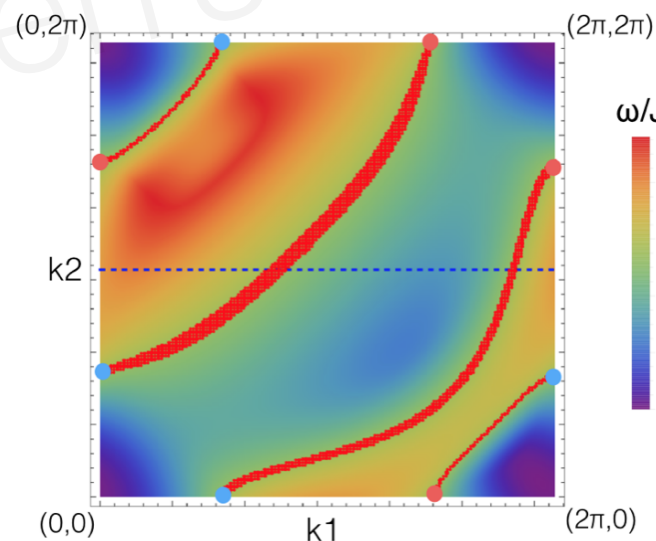
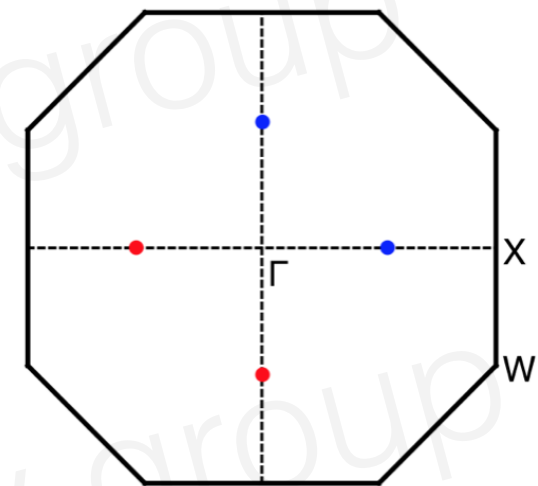
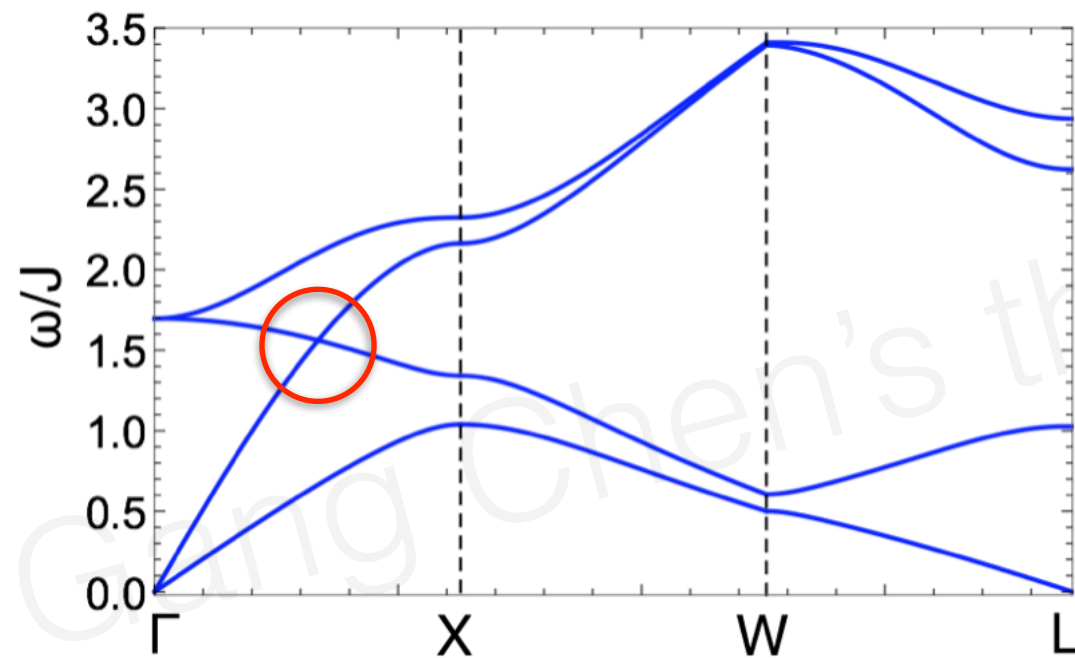
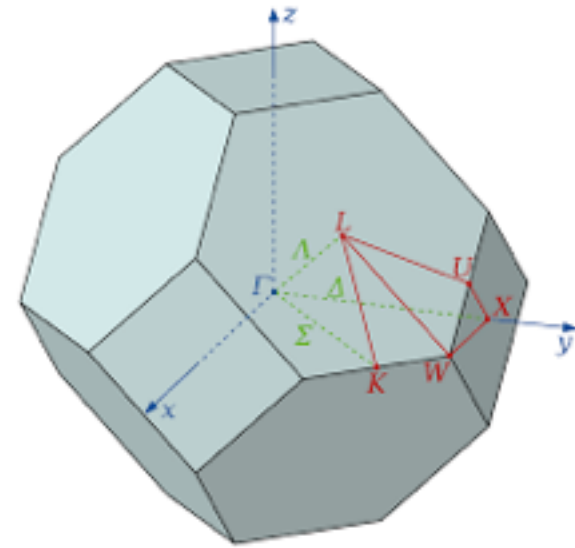
$$\mathbf{S}_i^{\text{cl}} \equiv S\hat{m}_i = S(\cos\theta \hat{x}_i + \sin\theta \hat{y}_i),$$

Holstein-Primarkoff bosons to express the spin operators as $\mathbf{S}_i \cdot \hat{m}_i = S - a_i^\dagger a_i$, $\mathbf{S}_i \cdot \hat{z}_i = (2S)^{1/2}(a_i + a_i^\dagger)/2$, and $\mathbf{S}_i \cdot (\hat{m}_i \times \hat{z}_i) = (2S)^{1/2}(a_i - a_i^\dagger)/(2i)$. Keeping terms in



I, II have the same order, but are distinct **topologically**!

Weyl magnons



surface arc states

(a)

(b)

Tune Weyl nodes with magnetic field

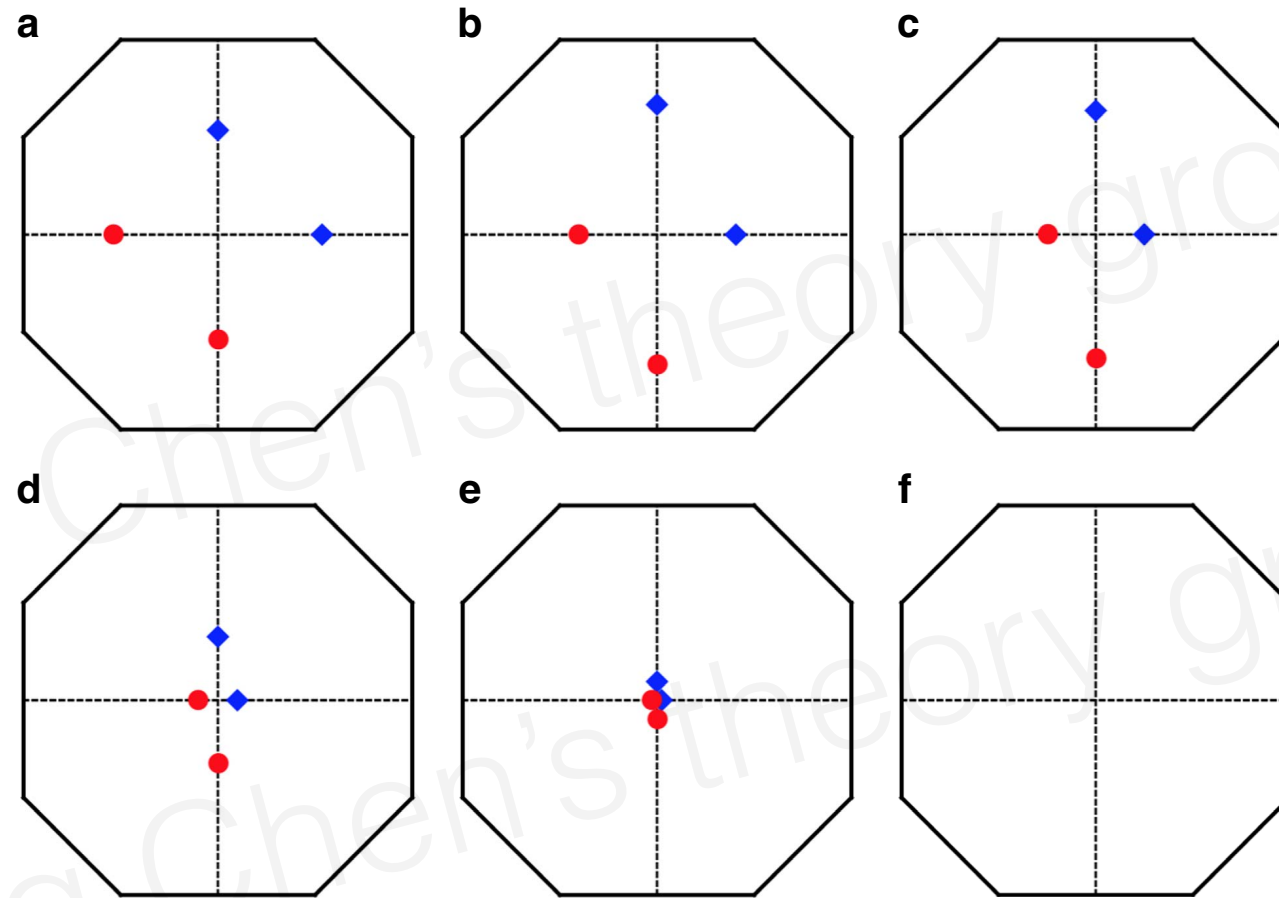


Figure 5 | The evolution of Weyl nodes under the magnetic field. Applying a magnetic field along the global z direction, $\mathbf{B}=B\hat{\mathbf{z}}$, Weyl nodes are shifted but still in $k_z=0$ plane. They are annihilated at Γ when magnetic field is strong enough. Red and blue indicate the opposite chirality. **(a,f)**: $B=0, 0.1J, 0.5J, 0.9J, 1.0J, 1.1J$. We have set $D=0.2J$, $J'=0.6J$ and $\theta=\pi/2$.

How to probe in a REAL experiment?

1. Neutron scattering: detect the Weyl nodes as well as the consequence (the surface arc states that connect the Weyl nodes).
2. Thermal Hall effect: magnon Weyl nodes contribute the thermal currents that are tunable by external magnetic field.
3. Optically: as Weyl node must appear at finite energy, one needs to use pump-probe measurement.

COMPARE TO Weyl fermion in the electron system

Extension

Dirac magnons (Yuan Li, Chen Fang, Jingsheng Wen) vs Dirac electron

nodal line magnon (??) vs nodal line semimetal

Magnon topological insulator vs electron topological insulator

Summary

We have studied a realistic spin model on the Cr-based breathing pyrochlore systems.

We show that the combination of the single-ion spin anisotropy and the superexchange interaction leads to conventional magnetic order.

We find the magnetic excitation in a large parameter regime develops magnon Weyl nodes in the magnon spectrum.